the most frequently used assumption is that of uniform flow at inlet, which simulates the actual condition of well-rounded entrance. This assumption was adopted in the present analysis and thus, at $x = 0$, the axial velocity and pressure are uniform with values u_0 and p_0, respectively.

Following the procedure suggested in [4], the nondimensional momentum equation in the axial direction can be written as:

$$\left(\frac{1+\alpha}{2\alpha}\right)^2 \frac{\partial U}{\partial X^*} + \frac{2}{\alpha}\left[\int_0^1 \frac{1}{R}\frac{\partial U}{\partial \theta}\bigg|_{\theta=0} dR - \int_0^\alpha \frac{\partial U}{\partial R}\bigg|_{R=1} d\theta\right]$$

$$= \frac{\partial^2 U}{\partial R^2} + \frac{1}{R}\frac{\partial U}{\partial R} + \frac{1}{R^2}\frac{\partial^2 U}{\partial \theta^2}, \qquad (1)$$

where $R = r/r_0$, $U = u/u_b$, $\epsilon(X) = dX/dX^*$, $X = x/(D_h Re)$, $D_h = 2r_0\alpha/(1+\alpha)$, $Re = D_h u_b/\nu$, and the parameter, ϵ can be formulated as:

$$\epsilon(X) = -\left[\frac{d}{dX^*}\int_A \left(U^2 - \frac{U^3}{2}\right)dA\right] \Big/ \int_A U\frac{\partial U}{\partial X^*}dA. \qquad (2)$$

The nondimensional pressure gradient is given by:

$$\left(\frac{1+\alpha}{\alpha}\right)^2 \frac{dP}{dX} = \frac{32}{\alpha}\int_A U\frac{\partial U}{\partial X}dA + \frac{16}{\alpha}\left[\int_0^1 \frac{1}{R}\frac{\partial U}{\partial \theta}\bigg|_{\theta=0} dR\right.$$

$$\left. + \int_0^\alpha \frac{\partial U}{\partial R}\bigg|_{R=1} d\theta\right], \qquad (3)$$

where $P = (p_0 - p)/(\frac{1}{2}\rho u_b^2)$. Appropriate boundary and symmetry conditions are:

$$U=0 \quad \text{at } R=1, 0\le\theta\le\alpha,$$
$$\text{and } \theta=0, 0\le R\le 1, \qquad (4a)$$

$$\text{and } \frac{\partial U}{\partial \theta}=0 \quad \text{at } \theta=\alpha, 0\le R\le 1. \qquad (4b)$$

Due to the symmetry around the plane $\theta = \alpha$, the solution need be carried out only over the region $0\le\theta\le\alpha$. Details of the derivation of equations (1)–(4) are given in [3].

Solutions were obtained using a finite difference aproach. At any axial location, the solution domain was subdivided by a 33 × 33 mesh, with the subdivisions adjacent to the straight and curved walls further subdivided into six equal parts for more accurate evaluation of wall gradients. The computation was marched from the inlet section to the fully developed region using axial steps with sizes $\Delta X^* = 1 \times 10^{-6}$ near the inlet, increasing to $\Delta X^* = 5 \times 10^{-4}$ as fully developed conditions were approached. Starting from the inlet section $X = X^* = 0$ where the value of U is given, the velocity distribution at $X^* = \Delta X^*$ was obtained by solving (1) interatively at all mesh points, subject to conditions (4). The value of ϵ was then obtained from (2) and the relation $\Delta X = \epsilon \Delta X^*$ was used for the evalution of ΔX. Finally, dP/dX was evaluated from (3) before marching to the next cross section. The solution was progressed until all axial velocities were within 1 percent of the corresponding fully developed value, and the value of X there was taken as the entrance length Le.

Numerical Results

The resulting values of Le are listed in Table 1 for the four duct geometries considered. With simple calculations, we can see from these results that for the same r_0, u_b, and ν, the entrance length increases as α increases. This trend is expected, however, quantitative comparisons are not possible due to lack of similar results. Development of the stretching factor ϵ along the duct is shown in Fig. 2 for different values of α. As shown in [3], the ϵ values for $\alpha = \pi/8$ compared well with those in [2]. The asymptotic value reached here for $\alpha = \pi/8$ is 1.92 as compared to 1.98 in [2]. It is also interesting to note that the present asymptotic values for ϵ (2.22 for $\alpha = \pi/32$, 2.03 for $\alpha = \pi/16$, 1.92 for $\alpha = \pi/8$, and 1.86 for $\alpha = \pi/4$) seem to conform with the asymptotic value of 1.82 obtained in [4] for smooth tubes. A sample of the velocity results illustrating the velocity development at the symmetry plane is shown in Fig. 3. The well-known characteristic of entrance region flow, namely that the fluid is decelerated near the walls and accelerated in the central core is clear from this figure. Again, our velocity results for $\alpha = \pi/8$ compared fairly well [3] with those in [2].

The most commonly used parameters for presenting the pressure results are the product of the friction factor and Reynolds number fRe, and the pressure defect K. In the present analysis, the friction factor was defined as:

$$f = (D_h/2)(-dp/dx)/(\rho u_b^2),$$

and hence

$$fRe = \frac{1}{4}\frac{dP}{dX} \qquad (5)$$

The pressure defect is normally defined as:

$$K(X) = [p_0 - p + (dp/dx)_{FD}x]/(\tfrac{1}{2}\rho u_b^2),$$

which reduces to the following nondimensional form:

$$K(X) = P - 4(fRe)_{FD}X. \qquad (6)$$

Results based on equations (5) and (6) are listed in Table 2. The values of fRe at $X = Le$ compare to within 3 percent of those reported in [1]. As expected [1], the present pressure results for $\alpha = \pi/8$ are widely different from those in [2]. A comparison between the K-values at $X = Le$ and the fully developed K-values reported in [1] is shown in Fig 4. It must be pointed out that the K_{FD} values reported in [1] are based on an approximate analytical method which utilizes only the fully developed velocity profile. Figure 4 shows a fair agreement with a maximum discrepancy of about 8 percent at $\alpha = \pi/32$.

Acknowledgments

The authors gratefully acknowledge the support provided for this research by the Natural Sciences and Engineering Research Council of Canada.

References

1 Shah, R. K., and London, A. L., *Laminar Flow Forced Convection in Ducts*, Academic Press, 1978.

2 Wendt, R. L., and Wiginton, C. L., "Incompressible Laminar Entrance Flow in a Circular Sector Duct," Journal of Applied Mechanics, Vol. 98, 1976, pp. 357–359.

3 Munis, A A., "Analysis of Laminar Fluid Flow in the Entrance Region of Circular Sector Ducts," M.Sc. Thesis, University of Manitoba, 1981.

4 Sparrow, E. M., Lin, S. H., and Lundgren, T. S., "Flow Development in the Hydrodynamic Entrance Region of Tubes and Ducts," *Physics of Fluids*, Vol. 7, 1964, pp. 338–347.

5 Sparrow, E. M., and Lin, S. H., "The Developing Laminar Flow and Pressure Drop in the Entrance Region of Annular Ducts," *Journal of Basic Engineering*, Vol. 86, 1964, pp. 827–834.

6 Fleming, D. P., and Sparrow, E. M., "Flow in the Hydrodynamic Entrance Region of Ducts of Arbitrary Cross-Section," ASME *Journal of Heat Transfer*, Vol. 91, 1969, pp. 345–354.

On Stochastic Dynamics of an Embedded Rigid Cylinder

A. Beltzer[1] and R. Parnes[2]

[1]Visiting Professor, School of Aerospace, Mechanical and Nuclear Engineering, University of Oklahoma at Norman, Norman, Okla. 73019. On leave from Holon Technical Institute, Israel. Mem. ASME.

[2]Associate Professor, Department of Solid Mechanics, Materials and Structures, School of Engineering, Tel-Aviv University, Ramat-Aviv, Israel.

Manuscript received by ASME Applied Mechanics Division, July, 1980; final revision, January, 1981.

Multidegree-of-freedom vibrations are considered for a rigid cylinder embedded in an isotropic elastic medium that is subjected to random propagating disturbances. The numerical results obtained enable one to select values of parameters of the system which would provide desirable motions of the inclusion.

1 Introduction

The classical linear theory of wave propagation provides a thorough analysis of the phenomenon of wave diffraction. However, this theory is concerned with traveling disturbances that are simple deterministic processes. It is well known that in reality these disturbances are usually random or incompletely defined. Due to this motivation, a number of investigations have been recently carried out on elastic and viscoelastic random waves. A survey of these works was presented by Beltzer [1].

This paper is concerned with random vibrations of an embedded rigid cylinder that are induced by elastic waves. All the stochastic processes used are taken to be stationary with zero mean. In view of the linearity of the system the last restriction does not lead to any loss of generality.

2 Basic Equations

We consider an infinite isotropic elastic medium (defined by its Lamé constants λ and μ and by its mass density ρ) which contains a rigid movable infinite cylinder with arbitrary radius a and mass density ρ_0. The medium is subjected to general plane waves of displacement traveling in the direction x and which impinge on the cylinder (Fig. 1).

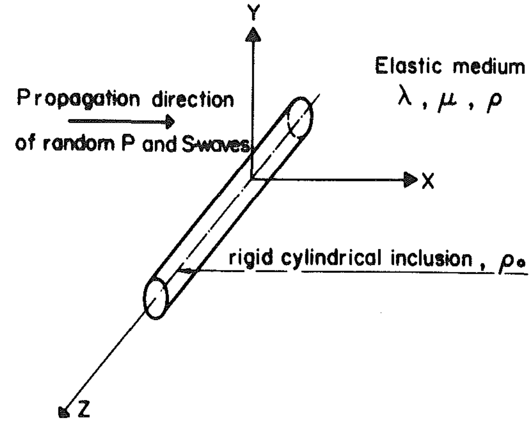

Fig. 1 Geometry of problem

The random motion of the cylinder under this impact is characterized by three degrees of freedom: displacements $u(t)$ and $v(t)$ in the directions x and y, respectively, and by a rotation $\phi(t)$ about the direction z. The displacement $u(t)$ is due to the P-component of the incident field only, whereas the SV-component causes both the displacements $v(t)$ and $\phi(t)$.

Let us denote the P or SV-component of the incident field of displacement as W_j ($j = p, s$), the spectrum of an incident wave as $Q_j(\omega)$, and the spectra of the inclusion motions as $\bar{Q}_k(\omega)$, $k = u, v, \phi$. Taking into account the separability mentioned between P and SV-waves of excitation and the components of the inclusion motion, one can write the following equations governing the steady-state response

$$\begin{Bmatrix} \bar{Q}_u(\omega) \\ \bar{Q}_v(\omega) \\ \bar{Q}_\phi(\omega) \end{Bmatrix} = \begin{bmatrix} |G_u^p(\omega)|^2 & 0 & 0 \\ 0 & |G_v^s(\omega)|^2 & 0 \\ 0 & 0 & |G_\phi^s(\omega)|^2 \end{bmatrix} \begin{Bmatrix} Q_p(\omega) \\ Q_s(\omega) \\ Q_s(\omega) \end{Bmatrix} \quad (1)$$

where $G_k^j(\omega)$, ($j = p, s$; $k = u, v, \phi$) is the cylinder displacement k due to normalized harmonic j-disturbance.

Making use of the results for the harmonic response of a rigid cylinder [2], we have the following expressions for $G_k^j(\omega)$

$$G_u^p(\omega) = i\eta[8H_1(\beta a) - 4\,\beta a\, H_0(\beta a)](\pi\alpha a\Delta)^{-1} \quad (2)$$

$G_v^s(\omega)$ is given by equation (2) where the replacements

$$\alpha \rightarrow \beta \quad \beta \rightarrow \alpha \text{ are made} \quad (3)$$

$$G_\phi^s(\omega) = 8\eta[\beta^2 a^2 H_1(\beta a) + 4\eta\beta a\, H_0(\beta a) - 8\eta H_1(\beta a)]^{-1}/(\pi a) \quad (4)$$

where

$$\Delta = 4\eta\, H_1(\alpha a) H_1(\beta a) - (1+\eta)\beta a\, H_0(\beta a)\, H_1(\alpha a)$$

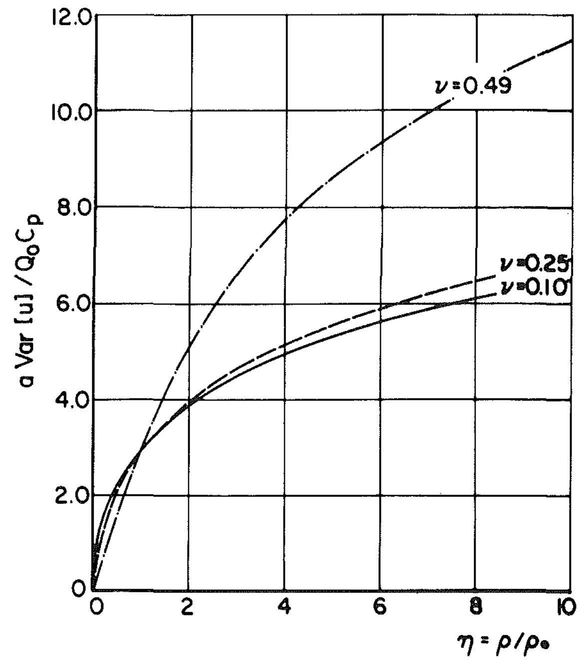

Fig. 2 Mean-square inclusion displacement in the x-direction versus density ratio η

$$-(1+\eta)\alpha a\, H_0(\alpha a)\, H_1(\beta a) + \alpha\beta\, a^2 H_0\,(\alpha a)\, H_0(\beta a) \quad (5)$$

and

$$\alpha = \omega/c_p; \quad \beta = \omega/c_s; \quad \eta = \rho/\rho_0 \quad (6)$$

In the foregoing $H_m(z) \equiv H_m^{(1)}(z)$ stands for the Hankel function of the first kind of the mth order and c_p and c_s are the velocities of dilatational and shear waves in the matrix.

Now we can determine the variances of nth derivatives of each of the stochastic processes of interest, i.e., of $u(t)$, $v(t)$, and $\phi(t)$

$$\text{Var}[k^{(n)}] = \int_{-\infty}^{\infty} \omega^{2n} \bar{Q}_k(\omega)\, d\omega, \quad (k = u, v, \phi; n = 0, 1, 2 \ldots) \quad (7)$$

3 Response to White Noise Disturbances

The spectra of the incident field is taken to be

$$Q_j(\omega) = Q_0 = \text{const}; \quad |\omega| < \infty, j = p, s \quad (8)$$

Making use of asymptotic expansions for $|G_k^j(\omega)|$ it can be shown that the improper integrals, given by equation 7, exist only for $n = 0$, i.e., for the variance of the displacements. The multivalued character of the Hankel

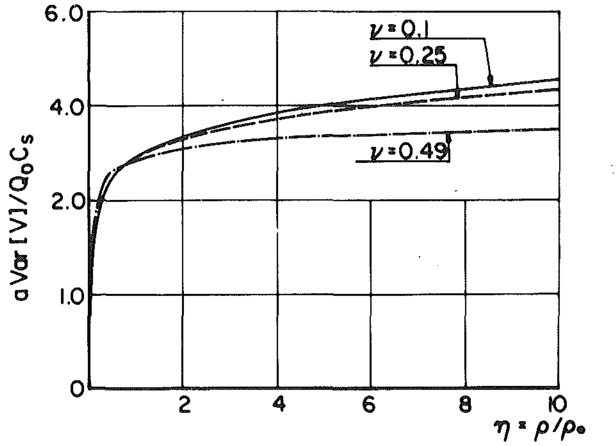

Fig. 3 **Mean-square inclusion displacement in the y-direction versus density ratio η**

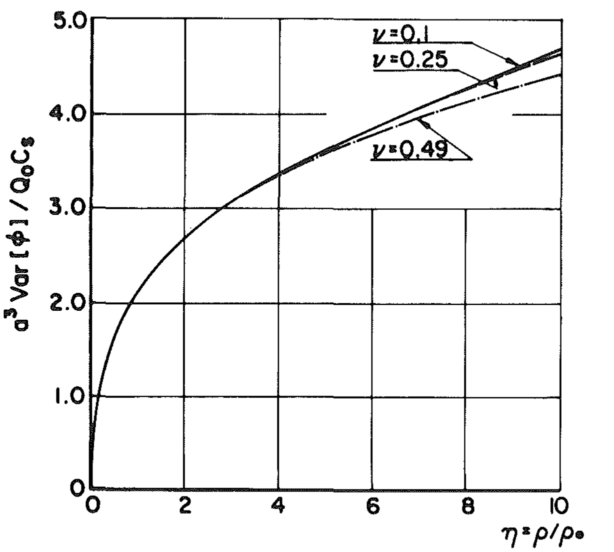

Fig. 4 **Mean-square inclusion rotation versus density ratio η**

functions necessitates a numerical evaluation of these integrals.

The results computed are presented in Figs. 2–4. As expected, these figures show that the motion of a "heavy" inclusion ($\eta < 1$) is always less random because of its greater inertia. The effect of the Poisson ratio, ν, on the variance of the inclusion motion is shown. For $\eta = 1$ the results are independent of ν for all components of the response. For other values of η, Var[u] and Var[v] are explicitly affected by this parameter whereas the influence on Var[ϕ] is slight. It is of interest to note that greater damping of the motion of a "light" inclusion ($\eta > 1$) in the y-direction occurs for a rubberlike material with $\nu \rightarrow 0.5$ as the matrix. On the other hand, for damping of the vibrations in the x-direction values as ν approaches zero are essentially more suitable (Figs. 2 and 3).

4 Conclusion

The results, presented in Figs. 2–4, cover the majority of practically interesting cases. They can be used in the analysis of composite materials to provide minimum (or maximum) damping or better protection of a rigid embedded cylinder. If the inclusion serves as a sensor for monitoring the incoming waves the results obtained can be employed to reduce the distortion due to a random noise.

References

1 Beltzer, A. I., "Random Waves in Solid Media," *The Shock and Vibration Digest*, Vol. 14, No. 3, 1982, pp. 3–6.

2 Pao, Y. H., and Mow, C. C., *Diffraction of Elastic Waves and Dynamic Stress Concentrations*, Crane Russak, New York, 1972.

On the Flow of a Viscoelastic Liquid Past an Infinite Porous Plate due to Fluctuation in the Main Flow

D. N. Mukhopadhyay[1] **and T. K. Chaudhury**[1]

Introduction

Stuart [1] and Messiha [2] investigated the oscillating flow of viscous liquid over an infinite flat plate with constant suction and variable suction, respectively, at the plate and discussed many interesting features of the flow. Soundalgekar and Puri [3] extended Messiha's problem to the case of non-Newtonian liquid with Walter's liquid B' [4] as the model. However the equations of motion considered by the authors [3] in the approximation of short relaxation time are identical with those of second-order liquid for the same problem and can be solved only by successive approximation. We extend Messiha's problem to the class of viscoelastic liquid known as stress-relaxing liquid of Oldroyd [5] and, as observed in our earlier work [6], we get a more general solution giving the solution [3] as a first approximation for small elastic parameter. Our solution shows some interesting effects of the stress-relaxing property of the liquid on the response of the boundary layer to the fluctuation in the main flow.

Formulation and Solution of the Problem

The constitutive equation for a viscoelastic liquid of Oldroyd [5] has the form

$$P_{ij} = -p\delta_{ij} + T_{ij},$$

$$T_{ij} + \lambda_1 \left(\frac{\partial T_{ij}}{\partial t} + v_K T_{ij,K} - v_{i,K} T_{Kj} - v_{J,K} T_{iK} \right) = 2\eta_0 e_{ij}, \qquad (1)$$

where P_{ij} and e_{ij} are, respectively, stress tensor and rate-of-strain tensor, v_i are velocity components, λ_1, is the relaxation time, and η_0 is the viscosity coefficient. Taking the x'-axis along the plate in the direction of flow and the y'-axis perpendicular to the plate directed into the liquid, the flow field is given by $u' = u'\ (y', t')$, $v' = v_0'\ (1 + \epsilon A e^{i\omega' t'})$, $\omega' = 0$ with the free stream velocity $U'(t')$ (cf., Messiha [2]), where v_0' is a nonzero constant mean suction velocity and A and ϵ are small positive constants such that $\epsilon A \leq 1$. The differential equation for u' will be obtained by elimination of stress component $T_{x'y'}$ between (1) and the momentum equation. This elimination is effected by taking the particular solution $T_{y'y'} = 0$, which means vanishing normal stress $T_{y'y'}$ at the line of entry (or exit) of the liquid through pores of the boundary.

Assuming external forces to be absent and introducing nondimensional quantities defined by $y = y' v_0'/\nu$, $t = v_0'^2 t/$

[1] Junior Research Fellow and Reader, respectively, Department of Mathematics, Burdwan University, Burdwan, West Bengal, India.

Manuscript received by ASME Applied Mechanics Division, April, 1981; final revision, December, 1981.